

2023-07-19

# May microbial ecological baseline exist in continental groundwater?

Zhong, S

<https://pearl.plymouth.ac.uk/handle/10026.1/21242>

---

10.1186/s40168-023-01572-4

Microbiome

Springer Science and Business Media LLC

---

*All content in PEARL is protected by copyright law. Author manuscripts are made available in accordance with publisher policies. Please cite only the published version using the details provided on the item record or document. In the absence of an open licence (e.g. Creative Commons), permissions for further reuse of content should be sought from the publisher or author.*

# 1 **May microbial ecological baseline exist in continental groundwater?**

2  
3 **Authors:** Sining Zhong<sup>1,2,3</sup>, Shungui Zhou<sup>3</sup>, Shufeng Liu<sup>1</sup>, Jiawen Wang<sup>1</sup>, Chenyuan  
4 Dang<sup>1</sup>, Qian Chen<sup>1,4</sup>, Jinyun Hu<sup>1</sup>, Shanqing Yang<sup>1</sup>, Chunfang Deng<sup>1</sup>, Wenpeng Li<sup>5</sup>, Juan  
5 Liu<sup>1</sup>, Alistair G.L. Borthwick<sup>6</sup>, Jinren Ni<sup>1,2\*</sup>

## 6 7 **Author affiliations:**

8 <sup>1</sup>College of Environmental Sciences and Engineering, Peking University; Key Laboratory  
9 of Water and Sediment Sciences, Ministry of Education, Beijing 100871, P. R. China

10 <sup>2</sup>State Environmental Protection Key Laboratory of All Material Fluxes in River  
11 Ecosystems, Beijing 100871, P. R. China

12 <sup>3</sup>Fujian Agriculture and Forestry University, College of Resources and Environment,  
13 Fujian Provincial Key Laboratory of Soil Environment Health and Regulation, Fuzhou  
14 350002, P. R. China

15 <sup>4</sup>State Key Laboratory of Plateau Ecology and Agriculture, Qinghai University, Xining  
16 810016, P. R. China

17 <sup>5</sup>Center for Groundwater Monitoring, China Institute of Geo-environmental Monitoring,  
18 Beijing 100081, P. R. China

19 <sup>6</sup>School of Engineering, Computing and Mathematics, University of Plymouth, Drake  
20 Circus, Plymouth PL8 4AA, UK.

21

22 **\*Corresponding author:** Jinren Ni

23 Postal address: Peking University, No. 5 Yiheyuan Road, Beijing 100871, P. R. China

24 Telephone number: +86-10-62751185

25 E-mail address: jinrenni@pku.edu.cn

26 **Abstract**

27 **Background:**

28 Microbes constitute almost the entire ecological community in subsurface groundwater  
29 and play an important role in ecological evolution and global biogeochemical cycles. As  
30 a fundamental benchmark independent of human interference, the concept of an  
31 ecological baseline has been investigated in surface ecosystems such as soils, rivers, and  
32 lakes, but the existence of a groundwater microbial ecological baseline (GMEB) has  
33 remained an open question to date.

34 **Results:** Based on high-throughput sequencing information derived from national  
35 monitoring of 733 newly constructed wells, we find that microbial communities in  
36 pristine groundwater exhibit a significant lateral diversity gradient, and gradually  
37 approach the topsoil microbial latitudinal diversity gradient with decreasing burial depth  
38 of phreatic water. Among 74 phyla dominated by *Proteobacteria* in groundwater,  
39 *Patescibacteria* act as keystone taxa that harmonize microbes in shallow aquifers and  
40 accelerate decline in bacterial diversity with increasing well-depth. Decreasing habitat  
41 niche breadth with increasing well-depth suggests a general change in the relationship  
42 among key microbes from close cooperation in shallow groundwater to strong  
43 competition in deep groundwater. Unlike surface-water microbes, microbial communities  
44 in pristine groundwater are predominantly shaped by deterministic processes, potentially  
45 associated with nutrient sequestration in a dark, anoxic environment.

46 **Conclusions:** By unveiling the biogeographic patterns and mechanisms controlling the

47 community assembly of microbes in pristine groundwater throughout China, we  
48 confirm the existence of a GMEB in shallow aquifers and propose a Groundwater  
49 Microbial Community Index (GMCI) to evaluate anthropogenic impact. GMCI highlights  
50 the importance of GMEB in groundwater water security and health diagnosis.

51

52 **Key Words:** GMEB, bacterial community, keystone taxa, deterministic processes,  
53 groundwater.

## 54 **Background**

55 Groundwater, the world's largest available store of freshwater resource, provides more  
56 than two billion people with drinking water and supplies approximately 40% of global  
57 irrigation [1]. Groundwater is vital to global biogeochemical cycles [2,3]. As the most  
58 ancient and diverse life form on Earth, microbes comprise almost the sole ecological  
59 community found in groundwater [4,5]. Over billions of years, groundwater microbes  
60 have participated in the metabolism of key elements such as carbon, nitrogen, sulfur,  
61 phosphorus, and various metals, and thereby have influenced the biogeochemistry of  
62 subsurface and even surface ecosystems [6,7]. Compared with the surface environment,  
63 aquifer ecosystems provide harsh habitats for biological survival due to their being devoid  
64 of photosynthesis, oxygen and readily available organic carbon [2,8], and so offer ideal  
65 targets for the study of microbial ecology, evolution, and environmental adaptation [9,10].  
66 In the past decade, the tree of life has significantly expanded owing to the discovery of  
67 vast previously uncharacterized and uncultured microbial populations in aquifers [11-13].  
68 For example, Brown et al. [11] newly defined >35 candidate phyla radiation  
69 (*Patescibacteria*), by reconstructing 789 draft genomes from groundwater samples. The  
70 superphylum *Patescibacteria* has received extensive attention, given its unique features  
71 of ultra-small cell size, small genome size, and lack of CRISPR, which helped facilitate  
72 a better understanding of the life of microbes in extreme environments [12,14]. Different  
73 assemblages of *Patescibacteria* organisms are key to turning the globally relevant  
74 subsurface biogeochemical cycles of carbon, nitrogen, sulfur, and hydrogen [15,16].

75 The ecological baseline delineates the original state of ecosystem attributes such as  
76 environmental parameters, biological composition, and service functions, and could be  
77 applied to the design of operational monitoring programs that quantify ecosystem change  
78 in response to anthropogenic disturbance and contamination[17,18]. Ecological baselines  
79 of soil, river, and ocean ecosystems established based on macro-organisms (e.g., fishes[19]  
80 and invertebrates[20]) have demonstrated that a return to the nearly original state could  
81 be expected upon the baselines being correctly determined and human interference being  
82 effectively controlled. Nowadays, groundwater is facing dual global threats to its water  
83 quality and quantity globally [21], and so an improved understanding is urgently needed  
84 of groundwater geochemistry and ecology in order to assess anthropogenic impact.  
85 Previous indices developed for groundwater ecological assessment, such as  
86 the groundwater quality index (WQI) [22], have invariably overlooked the significance  
87 of groundwater microbes. Meanwhile, the ubiquity, strong adaptability, and dispersal  
88 abilities of groundwater microbes have led to controversy as to whether or not microbial  
89 elements should be included in establishing the groundwater ecological baseline [23].  
90 Recent progress in advanced technologies, such as new generation high-throughput  
91 sequencing [24], has provided a means by which to uncover the mysterious world of  
92 microbes and facilitate exploration of the groundwater microbial ecological baseline  
93 (GMEB).

94 With the rapid development of high-throughput sequencing, numerous studies have  
95 established that microbes exhibit obvious microbial biogeographic patterns in a wide

96 variety of natural ecosystems, including terrestrial [25] and marine [26] systems.  
97 However, previous studies concerning groundwater ecosystems have been mostly limited  
98 to small scale, for example, contaminated areas [27], typical basins [28], and special  
99 geological zones [29], and so are unable to provide a holistic view of GMEB at large scale.  
100 Meanwhile, an understanding of the mechanisms that govern  
101 microbial community assembly is crucial for predicting the response of ecosystems to  
102 human activity. Several investigators have indicated that microbial biogeographic  
103 patterns are controlled by deterministic processes, including abiotic and biotic factors  
104 [27,30,31]. Such deterministic processes increase the predictability of microbial  
105 communities, providing theoretical support for the presence of a microbial ecological  
106 baseline. Other researchers have stressed the important roles of ecological drift, dispersal  
107 limit, and even historical contingency in community assembly [32,33]. Noting the  
108 significant habitat differentiation of complex heterogeneous environments in the  
109 subsurface, niche differentiation appears to offer a sensible ecological interpretation of  
110 variations in microbial diversity and composition [34,35].

111 Considering the severe scarcity of baseline data concerning the groundwater microbial  
112 ecosystem, we implemented a national monitoring campaign covering 733 newly  
113 constructed and 130 reconstructed wells across China (Fig. 1a) and established a unique  
114 microbial dataset, which has enabled us to address the following major questions: (1)  
115 Does GMEB exist at continental scale? (2) What are the lateral and vertical patterns of  
116 baseline microbial communities in different geo-environments? (3) What are the



117 dominators and keystone taxa in pristine groundwater? (4) Could the principal processes  
118 of community assembly be beneficial in shaping the GMEB? (5) Is there is a good index  
119 by which to assess the anthropogenic impact on groundwater based on the GMEB?

## 120 **Materials and methods**

### 121 **Study area and sample collection**

122 As the largest country in Asia, China has abundant groundwater resources distributed  
123 across various climatic belts and geo-environmental zones, and is ideal for exploring  
124 microbial communities in groundwater at continental scale. We obtained groundwater  
125 samples from 733 newly constructed wells and 130 reconstructed wells. In the newly  
126 constructed wells, sampling commenced immediately after exposure of groundwater to  
127 the external environment, thus providing first-hand samples useful as a baseline of  
128 groundwater microbes throughout China. Sampling from reconstructed wells enabled  
129 comparison with groundwater microbial communities in newly constructed wells,  
130 including 504 phreatic and 229 confined wells. The monitoring wells were distributed  
131 across seven geo-environmental zones covering 31 provinces in China (Fig. 1a, Table S1  
132 and S2). The sampling campaign occupied a wide geographical space extending from  
133 18.3°N to 52.0°N and from 76.1°E to 133.5°E. We focused on areas facing groundwater  
134 problems, such as the Beijing-Tianjin-Hebei region located in the Huanghuaihai-Yangtze  
135 River Delta Plain zone where the groundwater has experienced severe overexploitation  
136 and salinization.

137 Prior to sampling, groundwater in a given monitoring well was abstracted at a  
138 controlled discharge below 100 mL/min using a submersible sampling pump. Outflow  
139 water quality indicators (pH, electrical conductivity, oxidation-reduction potential, and  
140 turbidity) were measured using a portable tester (AP-800, Aquaread Ltd) at intervals  
141 ranging from 5 to 15 minutes until water quality stabilized over three consecutive  
142 measurements ( $\leq \pm 10\%$ ). More than 3,000 L of groundwater were drained from each  
143 sampling site and filtered by hollow fiber membranes to enrich microbial cells (Toray,  
144 0.01  $\mu\text{m}$ ). The hollow fiber membranes were transported with dry ice to designated  
145 laboratories and stored at  $-80\text{ }^{\circ}\text{C}$ .

146 Groundwater samples were collected in 5L sterile PET bottles for physicochemical  
147 content analysis. Prior to analysis, the samples were transported to the laboratory within  
148 12 h and stored at  $-4\text{ }^{\circ}\text{C}$ . According to the standard methods prescribed by the Ministry  
149 of Ecology and Environment of China, an array of physicochemical parameters, including  
150 total dissolved solids (TDS), chemical oxygen demand ( $\text{COD}_{\text{Mn}}$ ), ammonium nitrogen  
151 ( $\text{NH}_4^+\text{-N}$ ), and nitrate nitrogen ( $\text{NO}_3^-\text{-N}$ ), were determined. Key metal elements  
152 (including sodium (Na), potassium (K), calcium (Ca), and magnesium (Mg)) were  
153 measured by ICP-MS (Thermo Fisher Scientific, USA). Bicarbonate ( $\text{HCO}_3^-$ ) and  
154 Carbonate ( $\text{CO}_3^{2-}$ ) were measured using potentiometric titration, and Fluoride ( $\text{F}^-$ ),  
155 chloride ( $\text{Cl}^-$ ), and sulfate ( $\text{SO}_4^{2-}$ ) were determined by ion chromatography (Thermo  
156 Fisher Scientific, USA). All physicochemical parameters were normalized using Min-  
157 Max standardization.

158 **DNA extraction and bioinformatics analysis**

159 The substances captured by the hollow fiber membranes were dissolved in ultrapure water  
160 by ultra-sonication, then filtered through 0.22 µm polycarbonate membranes (Millipore,  
161 USA). Genomic DNA was extracted using the MoBio PowerSoil® kit (MoBio  
162 Laboratories, Carlsbad, CA, USA) according to manufacturer protocols. DNA quantity  
163 and quality (Table S3) were determined using a NanoDrop Spectrophotometer  
164 (NanoDrop Technologies Inc., Wilmington, DE, USA). Polymerase chain reaction (PCR)  
165 was used to amplify the V3-V4 hypervariable region of the bacterial 16S rRNA gene (3  
166 min at 95 °C, followed by 29 cycles at 95 °C for 30 s, 55 °C for 30 s, and 72°C for 45 s,  
167 and concluding with a final extension step at 72 °C for 10 min). Primers used for bacterial  
168 16S rRNA gene PCR amplification were 338F (5' -ACTCCTACGGGAGGCAGCAG-  
169 3' ) and 806R (5' -GGACTACHVGGGTWTCTAAT-3' ) [36]. Sequencing was  
170 performed by Shanghai Majorbio Bio-pharm Technology Company Ltd (Shanghai,  
171 China).

172 DNA sequences were quality-filtered on the Majorbio Cloud Platform  
173 (<https://cloud.majorbio.com/>) using QIIME v1.9.1 [37]. Operational taxonomic units  
174 (OTUs) were clustered with 97% similarity cutoff using UPARSE (version 7.1) [38], and  
175 chimeric sequences were identified and removed using UCHIME. A representative  
176 sequence of each OTU was selected for taxonomic assignment. Bacterial OTUs were  
177 assigned by the RDP classifier [39] against the SILVA 16S rRNA database  
178 (<http://www.arb-silva.de/>). A confidence threshold of 70% was used to analyze the

179 taxonomy for all OTUs. OTUs identified at the level of phylum, family, order, class, genus,  
180 and species were 86.7%, 80.4%, 61.6%, 38.3%, 23.9%, and 8.5%, respectively.

## 181 **Statistical analysis**

182 **Identification of the core microbial taxa (OTUs).** The core microbial taxa in  
183 groundwater were identified from the huge, unique datasets established **as part of** this  
184 study, following two criteria [40]. Firstly, we identified the most abundant OTUs based  
185 on average relative abundance  $< 0.01\%$ . Secondly, only ubiquitous OTUs occurring in  $>$   
186 50% of the total samples were considered. To identify the environmental preference of  
187 each core microbial taxa between newly constructed and reconstructed wells, the  
188 Wilcoxon rank-sum test was applied using the `wilcox.test` function in “stats” package in  
189 R version 3.6.1(<https://www.r-project.org/>). A similar test was conducted for core taxa  
190 between confined and phreatic groundwater in newly constructed wells. Sequences of  
191 core OTUs were compared with those archived in the National Center for Biotechnology  
192 Information (NCBI) nucleotide database, using the Basic Local Alignment Search Tool  
193 (BLAST) to obtain a more accurate phylogenetic tree. The closest sequences and selected  
194 reference sequences were aligned using ClustalW software. After alignment, gaps were  
195 trimmed with the trimAl tool (threshold = 0.2). The phylogenetic tree was constructed by  
196 the MEGA 7.0 tool using a neighbor-joining algorithm with a bootstrap test of 1000  
197 replicates and maximum composite likelihood model [41], and visualized using an online  
198 Interactive Tree Of Life server (<https://itol.embl.de/>).

199 **Alpha and beta diversity.** The OTU table for subsequent comparative analysis was

200 rarefied to the same sequencing depth (23976 sequences per sample). Alpha diversity was  
201 quantified using MOTHUR [42]. Taxonomic and phylogenetic diversities were measured  
202 using the Shannon diversity index and Faith's phylogenetic diversity. Linear and  
203 polynomial regression fits were constructed using the nlme R package. Non-metric  
204 multidimensional scaling (NMDS) was used to visualize the dissimilarity of beta diversity  
205 based on the Bray-Curtis distance. One-way analysis of variance (ANOVA) and Analysis  
206 of similarity (ANOSIM) were calculated to test the significance of differences in  
207 community diversity and structures among specific groups using the 'aov' and 'anosim'  
208 functions in vegan R package, respectively. Distance-decay relationships (DDRs) were  
209 calculated as the slopes of linear least-squares regressions for relationships between the  
210 natural logarithm of geographic distance and the natural logarithm of Bray-Curtis  
211 community similarity.

212 **Identification of biomarker.** Linear discriminant analysis effect size (LEfSe) was  
213 used with Wilcoxon and Kruskal-Wallis tests to discover high-dimensional biomarkers  
214 and explain taxa differences over varying well-depth ranges and geo-environmental zones.  
215 The LEfSe biomarker detection was performed in QIIME using the logarithmic LDA  
216 threshold  $> 3.5$  and the statistical parameters of  $P < 0.05$ .

217 **Network analysis.** Co-occurrence network analysis at genus level was performed to  
218 investigate the complex interactions among microbial communities for different well-  
219 depth ranges (0-20 m, 20-40 m, 40-60 m, 60-80 m, and  $> 80$  m). Firstly, rare genera with  
220 relative abundance of  $< 0.01\%$  were removed. Secondly, all possible Spearman's

221 correlation coefficients between two genera were calculated. Then, species pairs with  
222 strong (Spearman's  $|r| > 0.6$ ) and significant (FDR-adjusted  $P < 0.001$ ) correlations were  
223 selected to filter the data for reduced network complexity. Co-occurrence network  
224 visualization and modular analysis were conducted using the interactive platform Gephi  
225 (<http://gephi.github.io/>). The topology of networks (including average degree, average  
226 path length, clustering coefficient, graph density, and modularity) and node-level  
227 topological features (including degree, betweenness, and closeness centrality) were  
228 characterized using the igraph R package. Higher average degree, clustering coefficient,  
229 graph density, and lower average path lengths suggest a more connected co-occurrence  
230 network [43]. High mean degree, high closeness centrality, and low betweenness  
231 centrality were jointly used as thresholds for identifying keystone taxa [44].

232 **Niche breadth.** The niche breadth (B) index was estimated according to the formula  
233 [45]:

$$234 \quad B_j = 1 / \sum_{i=1}^N P_{ij}^2$$

235 where  $B_j$  indicates the niche breadth of species  $j$ ;  $P_{ij}$  is the proportion of species  $j$  present  
236 in habitat  $i$ . Species with a higher B-value are considered to be habitat generalists whereas  
237 species with a lower B-value are habitat specialists. Habitat niche breadths and mean  
238 niche breadths (OTUs) at community level were calculated as the summation and average  
239 of B-values of all taxa occurring in a single community[46].

240 **Ecological models.** **Fitness** of zero-sum multinomial (ZSM), pre-emption, broken stick,  
241 log-normal, Zipf, and Zipf–Mandelbrot models were employed to confirm whether niche

242 or neutral processes determined the community assembly within a sample. Akaike  
243 Information Criterion (AIC) values for the pre-emption, broken stick, log-normal, Zipf,  
244 and Zipf–Mandelbrot models were calculated using the ‘radfit’ function in the Vegan R  
245 package. The AIC value of ZSM model was determined using Tetame [47]. All models  
246 were compared based on their AIC values, with a lower AIC value indicating a better fit  
247 of the model to the sample [48]. The normalized stochasticity ratio (NST) was used to  
248 estimate ecological stochasticity of community assembly, with 50% taken as the boundary  
249 point between more deterministic (< 50%) and more stochastic (> 50%) assemblies  
250 [49,50]. NST values for microbial communities in different groundwater samples were  
251 calculated according to taxonomic and phylogenetic metrics using the NST R package.

252 **Influence of environmental variables.** Variation partitioning analysis (VPA) was  
253 conducted to address the relative roles of geographical and environmental factors and  
254 their combined effect on community variations, based on the Bray-Curtis distance [51].  
255 The Mantel test (999 permutations) was performed to examine the correlation between  
256 environmental variables and community structures. Environmental variables with  
257 variance inflation factors >10 were removed to ensure the absence of multicollinearity  
258 among environmental variables. Constrained correspondence analysis (CCA) of beta  
259 diversity with environmental variables was undertaken to investigate community  
260 distribution. VPA, Mantel test, and CCA were carried out using the vegan R package.  
261 Pearson and Spearman correlation analyses were performed using SPSS software (IBM  
262 Corporation, USA), and the corresponding heatmap plotted using the ggplots R package.

263 Detailed information on the grouping variables and statistical hypothesis for the analytical  
264 methods used in the study is provided in Table S4. Bonferroni correction p.adjust methods  
265 in the stats R package were used to provide strong control of the family-wise error rate.

266 **Groundwater Microbial Community Index (GMCI).** GMCI described the  
267 characteristic of microbial community by means of an integrated variable, analogous to  
268 and modified from the Invertebrate Community Index (ICI) [52] and Rapid Assessment  
269 Approach [20]. The procedure was as follows: (1) Construction of baseline data. Selection  
270 of the baseline sites as reference data must follow two principles, i.e., no-disturbance (or  
271 minimal level of anthropogenic interference) and relatively similar type of habitat to the  
272 monitoring site. (2) Selection of a subset of microbial indicators. Microbial diversity,  
273 dominators, key species, and biomarkers of pristine groundwater were selected as initial  
274 indicators. Any species with an occurrence rate less than 20% or average relative  
275 abundance less than 0.5% was excluded. (3) Observation and expectation ratio (O/E ratio)  
276 of microbial indicators was determined for the test sites. The 60% baseline and test  
277 samples were randomly selected to estimate the expectation value and set the alarm O/E  
278 ratio of each indicator, while each of the remaining samples was judged as to whether it  
279 had experienced strong anthropogenic interference by comparing its O/E ratio with the  
280 alarm O/E ratio. Indicators with low identified accuracy rate (accurate identified number  
281 / actual number of reconstructed wells) and high error rate (error identified number /  
282 actual number of newly constructed wells) would be eliminated. (4) Integration and  
283 calculation of GMCI. Multiple reliable indicators with weights and scores were integrated



284 into a single index namely GMCI. An alarm threshold value of GMCI = 1.0 was used to  
285 evaluate the status of each observed microbial community in groundwater, and the  
286 identified accuracy and error rate of anthropogenic interference then calculated.

## 287 **Results**

### 288 **Profiles of microbial communities in groundwater**

289 A total of 97,569 OTUs (operational taxonomic units sharing  $\geq 97\%$  sequence similarity),  
290 belonging to 74 phyla and 1703 genera, were obtained by high-throughput sequencing of  
291 groundwater samples acquired throughout China. Proteobacteria was the most abundant  
292 phylum (20.5% of the total OTUs and 52.1% of the total 16S rRNA sequences), followed  
293 by *Bacteroidota*, *Campilobacterota*, *Patescibacteria*, *Actinobacteriota*, *Firmicutes*,  
294 *Desulfobacterota*, *Chloroflexi*, *Acidobacteriota*, *Nitrospirota*, *Methylomirabilota*, and  
295 *Verrucomicrobiota* (Additional file 2: Fig. S1).

296 Similar to microbial communities in other systems [40,53], the species rank abundance  
297 distribution of groundwater microbes at national scale presented a typical peak-and-tail  
298 distribution (Additional file 2: Fig. S2), in which 1186 most abundant OTUs accounted  
299 for 74.9% of the total abundance, whereas 93.0% OTUs comprised regionally rare OTUs  
300 with a mean relative abundance of  $< 0.001\%$  [54]. Based on previous studies [40], we  
301 defined the core microbial taxa as OTUs of occurrence frequency  $> 50\%$  and mean  
302 relative abundance  $> 0.01\%$ . About 0.42% of OTUs (411) constituted the microbial core  
303 community in groundwater, accounting for 53.8% of the total abundance (Fig. 1b). Less

304 than 20% of the core OTUs matched an available reference genome at > 97% similarity  
305 level and 23.4% were uncultivated lineages. Most of the core OTUs belonged to  
306 *Proteobacteria* (*Gammaproteobacteria* and *Alphaproteobacteria*), *Actinobacteriota*,  
307 *Bacteroidota*, and *Firmicutes*. It is likely that these core taxa share certain phenotypic  
308 traits and/or life-history strategies to adapt to harsh subterranean habitats. For example,  
309 the genus *Pseudomonas* contained the most abundant and the largest number of core  
310 phylotypes in groundwater, which proved to have low nutritional requirements and a high  
311 diversity of energy metabolisms [55].

### 312 **Lateral and vertical pattern of baseline microbes**

313 Biogeographic patterns can provide important perspectives by which to understand  
314 ecological and evolutionary processes in a natural ecosystem [23]. Here we used  
315 Shannon's diversity index and Faith's phylogenetic diversity (PD) to derive  
316 biogeographic patterns of microbial alpha diversity in groundwater from 733 newly  
317 constructed wells across China. The taxonomic and phylogenetic diversities of  
318 groundwater microbes exhibited similar biogeographic patterns (Pearson's coefficient:  $r$   
319 = 0.85,  $P < 0.001$ ), peaking at mid-latitudes (around 40° N, Fig. 2a and 2b) with a clear  
320 increasing trend from west to east of China (Additional file 2: Fig. S3). Microbial  
321 diversity across the seven geo-environmental zones exhibited significant discrepancy  
322 (one-way ANOVA test:  $P < 0.001$ ) in phreatic water, highest in the Huanghuaihai-Yangtze  
323 River Delta Plain zone (II) and lowest in the South China Bedrock Foothill zone (III)  
324 (Additional file 2: Fig. S4). According to previous studies on the age-depth relationship

325 in groundwater [56], phreatic water could be further classified into several levels in terms  
326 of the range of well depth (e.g., 0-40 m, 40-80 m, and > 80 m). As the **well-depth** range  
327 decreased from > 80 m to 0-40 m, the latitudinal diversity gradient (LDG) in shallower  
328 groundwater ( $R^2 = 0.16$ ,  $P < 0.001$ ) **approached** the topsoil LDG pattern (Additional file  
329 1: **Table S5** and Additional file 2: Fig. 2c), and the vertical change gradient **was** especially  
330 obvious in eastern China (zone I, II, and III, Fig. 2d).

331 The distance-decay relationship (DDR) is regarded as a fundamental pattern in ecology  
332 [53,57]. The community similarity of groundwater microbes decreased significantly **as**  
333 **geographical** distance increased (Mantel  $r = 0.17$ ,  $P < 0.001$ ). Microbial communities  
334 between varying geo-environments displayed steeper DDR **slopes** (Additional file 2: Fig.  
335 S5, slope = -0.21) than those within individual geo-environmental zones (slope = -0.10),  
336 suggesting **an** apparent influence of regional hydrogeological factors on microbial  
337 communities in groundwater. This finding was further **confirmed** by **ANOSIM** test at the  
338 OTUs level ( $R_{\text{ANOSIM}} = 0.27$ ,  $P < 0.001$ ).

339 Given that the vertical layering of strata is known to be unique and complex [2], we  
340 explored the relationship between microbial communities and placing depth of wells. In  
341 comparison to more productive systems (e.g., topsoil) [25,58], microbial diversity in  
342 groundwater was much lower, and exhibited a declining trend with increasing burial depth  
343 under varying geo-geo-environments (Additional file 2: Fig. S6a and S7). This vertical  
344 trend was especially evident in phreatic water (Pearson's coefficient:  $r = 0.41$ ,  $P < 0.001$ ),  
345 compared with the irregular variation of microbial diversity in confined water ( $P > 0.05$ ).

346 Non-Metric Multidimensional Scaling (NMDS) analysis showed an obvious variation in  
347 microbial composition at OTUs level with well depth in phreatic water (Additional file 2:  
348 Fig. S6b), as confirmed by strong correlation between the second NMDS and well depth  
349 ( $r = -0.46$ ,  $P < 0.001$ ). Microbial communities in shallower phreatic water exhibited  
350 steeper DDR slope (0-40 m: slope= -0.18, Mantel  $r = 0.24$ ,  $P < 0.001$ ) and significantly  
351 higher  $\beta$  diversity ( $P < 0.001$ ) than in deeper phreatic water (>80 m: slope= -0.02, Mantel  
352  $r = 0.08$ ,  $P > 0.05$ ) (Additional file 2: Fig. S8).

### 353 **Biomarkers for depth-based microbial baselines in varying geo-environments**

354 To better understand the spatial heterogeneity of groundwater baseline microbial  
355 communities, we investigated the groundwater biomarkers in varying well-depth ranges  
356 (Fig. 3a) and geo-environmental zones (Fig. 3b and Fig. S9). Vertically, *Patescibacteria*,  
357 *Nitrospirota*, *Chloroflexi*, and *Methylomirabilota* preferred to occur in shallow  
358 groundwater (0-40 m), *Firmicutes* was more likely to appear in groundwater in the  
359 medium well-depth range (40-80 m), while *Proteobacteria* favored deeper groundwater  
360 (>80 m) and was the only phylum whose relative abundance increased significantly with  
361 well depth (Additional file 2: Fig. S10,  $r = 0.47$ ,  $P < 0.001$ ). In lateral space, we provided  
362 representative biomarkers for each geo-environment. For example, genus *Ralstonia* was  
363 found to be a suitable groundwater biomarker to distinguish between microbial  
364 communities in different geo-environmental regions, noting their much higher abundance  
365 in Qinghai-Tibet Plateau Alpine Frozen Soil zone (Fig. 3c).

366 As a superphylum of prevalent concern in recent years [14,16], *Patescibacteria* was

367 observed in more than 99.1% of groundwater samples, comprising 19.9% of the total  
368 OTUs (only second to *Proteobacteria*) and 5.7% of the total sequences (Additional file 2:  
369 Fig. S1). Relative abundance of *Patescibacteria* peaked in the Northeast Plain-Mountain  
370 zone (biomarker,  $10.7 \pm 1.3\%$ ) and **troughed** in the Northwest Arid Desert zone ( $1.1 \pm$   
371  $0.3\%$ ), mainly owing to habitat preferences of class *Parcubacteria* and *ABYI* (Additional  
372 file 2: Fig. S11b). *Patescibacteria* presented the most significant declining trend in  
373 relative abundance with increasing well depth in phreatic water (Additional file 2: Fig.  
374 S10, slope = - 0.36,  $r = -0.55$ ,  $P < 0.001$ ), and exhibited a positive correlation with  
375 groundwater microbial diversity (Additional file 2: Fig. S12,  $r = 0.56$ ,  $P < 0.001$ ). In  
376 general, the vertical variation in dominant taxa **appeared to weaken at** lower taxonomy  
377 levels (e.g., class, order, family, and genus) (Additional file 1: **Table S6**), confirming  
378 previous claims that distributed randomness was greater among similar functional taxa  
379 and niche differentiation was stronger for a local community[59]. However, certain  
380 classes of *Patescibacteria*, notably *Parcubacteria*, *Microgenomatia*, *Gracilibacteria*, and  
381 *Berkelbacteria*, exhibited significant **declines in** relative abundance with increasing well  
382 depth (Additional file 2: Fig S11c).

### 383 **Coexistent patterns of baseline microbes**

384 Microbial coexistent patterns in groundwater were **further investigated through the**  
385 **establishment of** co-occurrence networks based on microbial correlation relationships  
386 (Spearman's  $|r| > 0.6$  and FDR-adjusted  $P < 0.001$ ) **for** several well-depth ranges (Fig.  
387 4a). Microbes in deeper groundwater **exhibited** stronger interconnectivity than in

388 shallower groundwater, characterized by higher average degree, clustering coefficient,  
389 and graph density, but lower average path length of subnetwork [43] (Additional file 1:  
390 Table S7). Positive and negative interactions in a co-occurrence network have previously  
391 been found to reflect potential mutualistic and antagonistic relationships among microbes  
392 [60]. Significant negative correlation was found only in deeper groundwater (6.02%  
393 negative edges for well depths > 80 m) possibly due to stronger competition among  
394 interspecies in deeper groundwater, whereas mutualism or commensalism were more  
395 likely to occur in shallower groundwater.

396 Node-level topological metrics such as degree, closeness centrality, and betweenness  
397 centrality can be used to identify keystone taxa [44]. In Fig. 5, most nodes in networks  
398 belonged to *Proteobacteria* whose relative abundance tended to increase with increasing  
399 burial depth. However, the degree and closeness centrality of *Proteobacteria* members  
400 were significantly lower than that of *Patescibacteria* ( $P < 0.01$ ), implying a greater  
401 importance of *Patescibacteria* in maintaining structure and function of microbial  
402 communities in phreatic water. The keystone taxa largely belonged to the class *ABY1* and  
403 *Gracilibacteria* in shallow groundwater, with both having close connections with the taxa  
404 of *Proteobacteria*, *Chloroflexi*, *Dependentiae*, and *Verrucomicrobiota*. Whilst those in  
405 deep groundwater (> 80 m) seemed more diverse, with the majority of taxa being capable  
406 of adapting to extreme environmental conditions or subsistence on persistent organic  
407 pollutants; such as *Sphingomonas* which is capable of degrading polycyclic aromatic  
408 hydrocarbons [61].

409 **Groundwater microbial ecological baselines supported by deterministic processes**

410 To **provide supporting evidence for** GMEB, we assessed community assembly processes  
411 using several ecological models. Under the Akaike Information Criterion (AIC), we  
412 preliminarily confirmed the existence of GMEB by revealing the bacterial community  
413 assembly **that was** dominantly shaped by deterministic processes (Fig. 4a), with an  
414 exception of only 3.0% samples fitted to the ZSM model (neutral processes) [62]. This  
415 finding was further evidenced by the lower normalized stochasticity ratios [50] (NST <  
416 50%) of community assembly based on taxonomic (average 29.62%) and phylogenetic  
417 metrics (average 32.54%) (Additional file 1: **Table S8**). Moreover, community-level  
418 habitat and OTU-level mean niche breadths were used to **examine the variation in**  
419 groundwater microbial **diversity with** burial depth. In phreatic water, habitat niche  
420 breadths were higher than those in confined water ( $P < 0.001$ ), and exhibited an obvious  
421 declining trend with increasing burial depth (Pearson's coefficient:  $r = -0.35$ ,  $P < 0.001$ ;  
422 polynomial fit:  $R^2 = 0.12$ ,  $P < 0.001$ ) (Fig. 5b), further confirmed the **increased**  
423 competition among microbes for survival resource and space in deeper groundwater.  
424 Conversely, the mean niche breadths in phreatic water were significantly lower than in  
425 confined water ( $P < 0.001$ ), and demonstrated a strongly positive correlation with well  
426 depth (Pearson's coefficient:  $r = 0.28$ ,  $P < 0.001$ ; polynomial fit:  $R^2 = 0.13$ ,  $P < 0.001$ )  
427 (Fig. 5c), suggesting the significance of niche differentiation in shaping groundwater  
428 microbial ecological baseline pattern.

429 We performed variance partition analysis (VPA) based on Bray-Curtis similarity to

430 evaluate the relative importance of environmental selection in groundwater microbial  
431 community assembly. Overall, the environmental variables provided a much more  
432 detailed picture of the spatial variation of the microbial community, particularly in  
433 shallow phreatic water (0-40 m, 15.27%, Additional file 2: Fig. S8b). Among the 58  
434 parameters considered, the Mantel test suggested a relatively higher correlation between  
435 microbial structures and chemical oxygen demand (COD), Manganese (Mn), and  
436 bicarbonate ( $\text{HCO}_3^-$ ) in groundwater (Additional file 2: Fig. S13). Canonical  
437 correspondence analysis (CCA) further indicated that geochemical signatures represented  
438 by  $\text{Na}^+$ ,  $\text{K}^+$ ,  $\text{Cl}^-$ , and  $\text{HCO}_3^-$ , which were closely related to the hydrogeological conditions  
439 in varying geo-environmental zones, had significant impact on the distribution of  
440 groundwater microbes (Additional file 2: Fig. S14).

## 441 Discussion

442 Ecological baselines are essential for reconciling arguments about maintenance of  
443 biological diversity, original state of biotic communities, and ecosystem functions [63].  
444 The existence of ecological baseline on subsurface groundwater is still an important and  
445 open question due to the extreme susceptibility to pollution. The concept of a groundwater  
446 microbial ecological baseline (GMEB) is an extension of the ecological baseline of earth  
447 surface ecosystems [17,18], and is proposed specifically for subsurface groundwater  
448 ecosystems where microbes are almost the only organisms present [64]. We define the  
449 GMEB as a reference for comparing microbial communities in groundwater affected by  
450 human intervention with those in the absence of human intervention. The GMEB has four



451 unique characteristics: (1) the GMEB should be in pristine groundwater and thus derived  
452 from “newly constructed wells” to avoid (as far as possible) interference from human  
453 activities; (2) the GMEB should be capable of representing the entire bacterial community  
454 including uncultured bacterial species, through the use of advanced high-throughput  
455 sequencing technology; (3) the GMEB should be determined using sufficient samples  
456 taken from representative sites covering a typical variety of hydrological and geological  
457 environments at continental scale; and (4) the GMEB should be largely driven by  
458 deterministic processes in terms of specific niche. In the present work, we implemented  
459 a large-scale monitoring campaign to obtain first-hand data from “newly constructed  
460 wells” to establish the GMEB and parallel data from “reconstructed wells” to evaluate  
461 anthropogenic impacts on microbial community structures at the test sites. The stability  
462 of microbial communities in groundwater has been proved spatiotemporally with the  
463 proviso that habitats remained unchanged [65,66]. The higher community similarity  
464 within the same geo-environment and its significant distance decay in pristine  
465 groundwater throughout China supports the fundamental assumption that similar  
466 biological components should be expected at congeneric environments in the absence of  
467 human intervention [20].

468 Recent progress in high-throughput sequencing has provided us with a relatively  
469 unbiased compositional snapshot of microbial communities [24], and helped us uncover  
470 the mysterious world of subsurface microbes. Based on the present unique bacterial  
471 dataset derived from pristine groundwater, we depicted the baseline patterns by

472 comparing the microbial latitude diversity gradient in pristine groundwater at different  
473 burial depths and in the topsoil. Laterally, baseline microbes exhibited a unimodal LDG  
474 pattern with highest diversity at latitudes close to 40°N, suggesting mid-latitude of high  
475 humidity and warm temperature would provide optimum survival habitats for microbes.  
476 Vertically, the LDG approached those in the topsoil with decreasing burial depth [25,58],  
477 indicating the divergent microbial pool at the surface would directly influence microbial  
478 diversity in shallow groundwater. In short, the geo-environment, as a complex  
479 macroscopic factor controlling hydrological connectivity and chemical characteristics of  
480 groundwater, has played an important role in shaping the biogeographic patterns of  
481 baseline microbes across China. Groundwater microbial diversity is highest in the  
482 Huanghuaihai-Yangtze River Delta Plain zone due to relatively frequent surface-  
483 groundwater interactions promoted by local hydrogeological characteristics including  
484 multi-fault structures, widespread loose and non-rock clay accumulation, and slow  
485 horizontal runoff [67].

486 Microbial ecological baseline patterns in pristine groundwater might be primarily  
487 mediated by certain dominant and key taxa [68]. *Proteobacteria*, the most typical habitat  
488 generalists [45], were confirmed as absolute dominators of groundwater microbial  
489 community. Driven by the mass propagation of their few taxa, *Proteobacteria* tended to  
490 have greater relative abundance in extreme environments, which would in turn inhibit  
491 local microbial diversity (Fig. S11,  $r = -0.54$ ,  $P < 0.001$ ). On the other hand, the majority  
492 of *Patescibacteria* members exhibited niche specialization and demonstrated significant

493 declines in relative abundance and diversity with increasing well depth. *Patescibacteria*  
494 were characterized by small genome size, presence of potential attachment and adhesion  
495 proteins, and absence of numerous biosynthetic capacities, suggesting that they could not  
496 live alone and instead **would** be parasites or form mutualistic arrangements with other  
497 microorganisms [15,16]. Network analysis further revealed the mediating role of  
498 *Patescibacteria* as keystone taxa in shallow phreatic water (Fig. 5b). Through anaerobic  
499 fermentative metabolism, certain members of *Patescibacteria* were capable of producing  
500 organic carbon, including hydrogen, acetate, formate, and ethanol, for other microbes  
501 [12,14]. Moreover, *Patescibacteria* may promote and maintain the interconnectedness  
502 and connectivity of the microbial community via quorum sensing signals and potential  
503 co-metabolism[69]. Some phylotypes of *Patescibacteria* were unable to colonize  
504 successfully in absence of available symbiotic partners **because of the** scarcity of  
505 available niches, further accelerating decline in microbial diversity in **deep phreatic-water**  
506 **layers beyond the scope of the present study aimed at establishing a groundwater**  
507 **microbial baseline.**

508 **The existence of a GMEB relies on niche differentiation with respect to microbes in**  
509 **pristine groundwater, implying the importance of deterministic processes in community**  
510 **assembly [34]. In surface water, microbial communities tend to be driven by stochastic**  
511 **processes due to strong flow-induced turbulence [70]. In pristine groundwater however,**  
512 **microbial communities are predominantly shaped by deterministic processes controlled**  
513 **by relatively isolated, stable, highly heterogeneous habitats, leading to the possible**

514 occurrence of a GMEB. The persistent selection march according to subterranean  
515 environmental constraints would preserve microorganisms capable of efficient energy  
516 utilization and/or special strategies of nutrient sequestration which cope better in  
517 conditions of low energy flux [6,71]. Our study has indicated that a relatively high  
518 proportion of autotrophic microbes can exist in groundwater, being strongly influenced  
519 by specific electron acceptors or donors (e.g.,  $\text{HCO}_3^-$ , Fe, Mn, and nitrate) (Additional  
520 file 2: Fig. S15). These findings partially explain how microbial communities adapt to  
521 subterranean dark, anoxic, nutrient - limited environments. From the perspective of  
522 assessing anthropogenic impact on groundwater ecosystems, shallow phreatic water  
523 should be of much greater significance for the establishment of GMEB given its ready  
524 susceptibility to human interference. Interestingly, environmental selection has been  
525 found to provide a relatively poorer explanation of microbial community variation in deep  
526 phreatic or confined water, but this does not affect the claim about existence of a microbial  
527 baseline in shallow phreatic water (Additional file 2: Fig. S16). Beyond the scope of  
528 shallow phreatic water, a higher mean niche breadth of taxa has been observed due to  
529 increased proportions of habitat generalists with high biological adaptability through a  
530 long-term series of ecological successions [45], ultimately leading to relatively low  
531 diversity and high community homogeneity in deep groundwater.

532 Subterranean microbes are particularly sensitive to anthropogenic intervention in their  
533 evolutionary adaptations [72]. The GMEB suggests that similar microbial structures  
534 should be expected at congeneric environments in the absence of human intervention.

535 Therefore, the anthropogenic impact on microbial community structures in the test sites  
536 could be evaluated by comparing with the baseline at reference sites **with** similar habitats  
537 [17,18]. At a national scale, our monitoring results **have** indicated that anthropogenic  
538 perturbation did cause an increase in microbial diversity and alteration of community  
539 structure even at phylum level (Additional file 2: Fig. S17). To facilitate evaluation of  
540 anthropogenic impact in practical groundwater monitoring, we proposed Groundwater  
541 Microbial Community Index (GMCI), which integrated microbial diversity, key species,  
542 and biomarkers (see Methods). **For  $GMCI \geq 1.0$ , the anthropogenic impact would be**  
543 **significant at specific test sites matched against the same reference group (Additional file**  
544 **1: Table S9, S10, and S11), with larger GMCI index indicating a stronger effect of human**  
545 **activity. To fully understand the effects of human activities on microbial ecological**  
546 **baselines in groundwater, we devised two categories of microbial baseline: one is the**  
547 **baseline at reference sites in regions **experiencing** intensive human intervention, **such as****  
548 **the Beijing region, and the other is in regions with less human interference, **such as the****  
549 **Xinjiang region. Without loss of generality, the difference in monitored community**  
550 **dissimilarity between newly constructed and reconstructed wells (Fig. 6a and Additional**  
551 **file 2: Fig. S18) in these two representative regions corresponded to the GMCI-based**  
552 **assessment results (Fig. 6b). It should be noted that the GMCI-based assessment had some**  
553 **obvious drawbacks. For example, the sequencing depth and sampling methods**  
554 **significantly influenced the resolution and accuracy of high-throughput sequencing,**  
555 **which required us to formulate standard monitoring methods for microbial communities.**

556 Noting the present inadequacy of GMCI data, priority should be given to the classification  
557 of reference groups and construction of a reference database for typical microbial habitats.

## 558 **Conclusions**

559 We confirmed the existence of the GMEB at continental scale by unveiling the  
560 biogeographic pattern of microbes in pristine phreatic water based on a unique dataset  
561 derived from recent monitoring of 733 newly constructed wells in seven geo-  
562 environmental zones across China. The GMEB exhibits a latitudinal diversity gradient  
563 pattern which approximates that in topsoil with decreasing well depth, and the alpha  
564 diversity peaks in the belt around 40°N due to frequent groundwater-surface interactions  
565 facilitated by special geo-environments. We found that *Proteobacteria* was the dominator  
566 (contributing over half the total abundance) in groundwater, while *Patescibacteria* acted  
567 as hubs harmonizing symbiotic microbes in shallower phreatic aquifers and promoting  
568 the vertical decay of microbial communities downwards. We revealed the endogenous  
569 mechanism for microbial co-occurrence in shallower phreatic water, and the ideal  
570 exogenous conditions for baseline microbes predominantly driven by deterministic  
571 processes under varying geo-environments. Furthermore, we proposed GMCI-based  
572 assessment to facilitate evaluation of anthropogenic impact in practical groundwater  
573 monitoring, highlighting the fundamental importance of GMEB for health diagnosis and  
574 water security of underexplored groundwater ecosystems. In the long run, much more  
575 information is needed to enrich the reference database and continuously improve the  
576 system of reference groups constituted by microbes and their matched habitats.

577 Multimeric approaches need to be developed that account for the combined effect of  
578 multiple attributes and provide an overall evaluation of the status of the microbial  
579 community under severe anthropogenic interference. In this regard, the concept of a  
580 “habitat ~ microbial reference ~ subterranean truth” system is recommended to reflect the  
581 relationship between geo-environment and microbial structure in groundwater  
582 ecosystems at regional, national, and global scales.

583

#### 584 **Acknowledgements**

585 We are grateful for support from Majorbio Company (Shanghai, China) and Geo-cloud  
586 Database of China Geological Survey.

#### 587 **Authors’ contributions**

588 J.R.N. designed the research. S.N.Z performed the research with help of C.Y.D., Q.C.,  
589 J.Y.H., and C.F.D., S.N.Z, A.G.L.B. and J.R.N. wrote the paper. All authors contributed  
590 new ideas and participated in interpretation of the findings.

#### 591 **Funding**

592 Financial support is from the National Natural Science Foundation of China under  
593 Grant Nos 51721006 and 91647211.

#### 594 **Availability of data and materials**

595 All the raw datasets supporting the findings of this article are available in the NCBI

596 Sequence Read Archive under BioProject number PRJNA692269.

597

598 **Declarations**

599 **Ethics approval and consent to participate**

600 Not applicable.

601 **Consent for publication**

602 Not applicable.

603 **Competing interests**

604 The authors declare that they have no competing interests.

605



## 606 **References**

- 607 1 de Graaf IEM, Gleeson T, van Beek LPH, Sutanudjaja EH, Bierkens MFP. Environmental flow limits  
608 to global groundwater pumping. *Nature*. 2019; 574: 90-94.
- 609 2 Griebler C, Lueders T. Microbial biodiversity in groundwater ecosystems. *Freshw. Biol.* 2009; 54: 649-  
610 677.
- 611 3 McDonough LK, Santos IR, Andersen MS, O'Carroll DM, Rutledge H, Meredith K, et al. Changes in  
612 global groundwater organic carbon driven by climate change and urbanization. *Nat. Commun.* 2020;  
613 11: 1279.
- 614 4 Whitman WB, Coleman DC, Wiebe WJ. Prokaryotes: The unseen majority. *Proc. Natl. Acad. Sci. U. S.*  
615 *A.* 1998; 95: 6578-6583.
- 616 5 Magnabosco C, Lin LH, Dong H, Bomberg M, Ghiorse W, Stan-Lotter H, et al. The biomass and  
617 biodiversity of the continental subsurface. *Nat. Geosci.* 2018; 11: 707-720.
- 618 6 Probst AJ, Ladd B, Jarett JK, Geller-McGrath DE, Sieber CMK, Emerson JB, et al. Differential depth  
619 distribution of microbial function and putative symbionts through sediment- hosted aquifers in the deep  
620 terrestrial subsurface. *Nat. Microbiol.* 2018; 3: 328-336.
- 621 7 Wang S, Zhu G, Zhuang L, Li Y, Liu L, Lavik G, et al. Anaerobic ammonium oxidation is a major N-  
622 sink in aquifer systems around the world. *ISME J.* 2019; 14: 151-163.
- 623 8 Chiriac CM, Baricz A, Szekeres E, Rudi K, Dragos N, Coman C. Microbial Composition and Diversity  
624 Patterns in Deep Hyperthermal Aquifers from the Western Plain of Romania. *Microb. Ecol.* 2018; 75:  
625 38-51.
- 626 9 Hubalek V, Wu X, Eiler A, Buck M, Heim C, Dopson M, et al. Connectivity to the surface determines  
627 diversity patterns in subsurface aquifers of the Fennoscandian shield. *ISME J.* 2016; 10: 2447-2458.
- 628 10 Seyler LM, Trembath-Reichert E, Tully BJ, Huber JA. Time-series transcriptomics from cold, oxic  
629 subseafloor crustal fluids reveals a motile, mixotrophic microbial community. *ISME J.* 2021; 15: 1192-  
630 1206.
- 631 11 Brown CT, Hug LA, Thomas BC, Sharon I, Castelle CJ, Singh A, et al. Unusual biology across a group  
632 comprising more than 15% of domain Bacteria. *Nature*. 2015; 523: 208-U173.
- 633 12 Anantharaman K, Brown CT, Hug LA, Sharon I, Castelle CJ, Probst AJ, et al. Thousands of microbial  
634 genomes shed light on interconnected biogeochemical processes in an aquifer system. *Nat. Commun.*  
635 2016; 7: 13219.
- 636 13 Hug LA, Baker BJ, Anantharaman K, Brown CT, Probst AJ, Castelle CJ, et al. A new view of the tree  
637 of life. *Nat. Microbiol.* 2016; 1: 16048.
- 638 14 He C, Keren R, Whittaker ML, Farag IF, Doudna JA, Cate JHD, et al. Genome-resolved metagenomics  
639 reveals site-specific diversity of episymbiotic CPR bacteria and DPANN archaea in groundwater  
640 ecosystems. *Nat. Microbiol.* 2021; 6: 354-365.
- 641 15 Lemos LN, Medeiros JD, Dini-Andreote F, Fernandes GR, Varani AM, Oliveira G, et al. Genomic  
642 signatures and co-occurrence patterns of the ultra-small Saccharimonadia (phylum CPR/Patescibacteria)  
643 suggest a symbiotic lifestyle (vol 28, pg 4259, 2019). *Mol. Ecol.* 2020; 29: 1936-1936.
- 644 16 Tian R, Ning D, He Z, Zhang P, Spencer SJ, Gao S, et al. Small and mighty: adaptation of superphylum  
645 Patescibacteria to groundwater environment drives their genome simplicity. *Microbiome.* 2020; 8: 51.
- 646 17 Burger J, Gochfeld M, Powers CW, Greenberg M. Defining an ecological baseline for restoration and

- 647 natural resource damage assessment of contaminated sites: The case of the department of energy. *J.*  
648 *Environ. Plan. Manag.* 2007; 50: 553-566.
- 649 18 Linder HL, Horne JK, Ward EJ. Modeling baseline conditions of ecological indicators: Marine  
650 renewable energy environmental monitoring. *Ecol. Indic.* 2017; 83: 178-191.
- 651 19 Hobday AJ. Sliding baselines and shuffling species: implications of climate change for marine  
652 conservation. *Mar. Ecol.-Evol. Persp.* 2011; 32: 392-403.
- 653 20 Lei L, Sun JS, Borthwick AGL, Fang Y, Ma JP, Ni JR. Dynamic Evaluation of Intertidal Wetland  
654 Sediment Quality in a Bay System. *J. Environ. Inform.* 2013; 21: 12-22.
- 655 21 Griebler C, Avramov M. Groundwater ecosystem services: a review. *Freshw. Sci.* 2015; 34: 355-367.
- 656 22 Khanoranga, Khalid S. An assessment of groundwater quality for irrigation and drinking purposes  
657 around brick kilns in three districts of Balochistan province, Pakistan, through water quality index and  
658 multivariate statistical approaches. *J. Geochem. Explor.* 2019; 197: 14-26.
- 659 23 Meyer KM, Memiaghe H, Korte L, Kenfack D, Alonso A, Bohannan BJM. Why do microbes exhibit  
660 weak biogeographic patterns? *ISME J.* 2018; 12: 1404-1413.
- 661 24 Reuter JA, Spacek DV, Snyder MP. High-throughput sequencing technologies. *Mol. Cell.* 2015; 58:  
662 586-597.
- 663 25 Bahram M, Hildebrand F, Forslund SK, Anderson JL, Soudzilovskaia NA, Bodegom PM, et al.  
664 Structure and function of the global topsoil microbiome. *Nature.* 2018; 560: 233-237.
- 665 26 Sunagawa S, Coelho LP, Chaffron S, Kultima JR, Labadie K, Salazar G, et al. Structure and function  
666 of the global ocean microbiome. *Science.* 2015; 348: 1261359.
- 667 27 Carlson HK, Price MN, Callaghan M, Aaring A, Chakraborty R, Liu H, et al. The selective pressures  
668 on the microbial community in a metal-contaminated aquifer. *ISME J.* 2019; 13: 937-949.
- 669 28 Wang L, Yin Z, Jing C. Metagenomic insights into microbial arsenic metabolism in shallow  
670 groundwater of Datong basin, China. *Chemosphere.* 2020; 245: 125603.
- 671 29 Mikucki JA, Auken E, Tulaczyk S, Virginia RA, Schamper C, Sorensen KI, et al. Deep groundwater  
672 and potential subsurface habitats beneath an Antarctic dry valley. *Nat. Commun.* 2015; 6: 6831.
- 673 30 Power JF, Carere CR, Lee CK, Wakerley GLJ, Evans DW, Button M, et al. Microbial biogeography of  
674 925 geothermal springs in New Zealand. *Nat. Commun.* 2018; 9: 16.
- 675 31 Liu S, Wang H, Chen L, Wang J, Zheng M, Liu S, et al. Comammox nitrospira within the Yangtze River  
676 continuum: community, biogeography, and ecological drivers. *ISME J.* 2020; 14: 2488-2504.
- 677 32 Archer SDJ, Lee KC, Caruso T, Maki T, Lee CK, Carys SC, et al. Airborne microbial transport limitation  
678 to isolated Antarctic soil habitats. *Nat. Microbiol.* 2019; 4: 925-932.
- 679 33 Fodelianakis S, Moustakas A, Papageorgiou N, Manoli O, Tsikopoulou I, Michoud G, et al. Modified  
680 niche optima and breadths explain the historical contingency of bacterial community responses to  
681 eutrophication in coastal sediments. *Mol. Ecol.* 2017; 26: 2006-2018.
- 682 34 Pernthaler J. Competition and niche separation of pelagic bacteria in freshwater habitats. *Environ.*  
683 *Microbiol.* 2017; 19: 2133-2150.
- 684 35 Welch JLM, Ramirez-Puebla ST, Borisy GG. Oral Microbiome Geography: Micron-Scale Habitat and  
685 Niche. *Cell Host Microbe.* 2020; 28: 160-168.
- 686 36 Caporaso JG, Lauber CL, Walters WA, Berg-Lyons D, Lozupone CA, Turnbaugh PJ, et al. Global  
687 patterns of 16S rRNA diversity at a depth of millions of sequences per sample. *Proc. Natl. Acad. Sci.*  
688 *U. S. A.* 2011; 108: 4516-4522.
- 689 37 Caporaso JG, Kuczynski J, Stombaugh J, Bittinger K, Bushman FD, Costello EK, et al. QIIME allows

690 analysis of high-throughput community sequencing data. *Nat. Methods*. 2010; 7: 335-336.

691 38 Edgar RC. UPARSE: highly accurate OTU sequences from microbial amplicon reads. *Nat. Methods*.  
692 2013; 10: 996-998.

693 39 Wang Q, Garrity GM, Tiedje JM, Cole JR. Naive Bayesian classifier for rapid assignment of rRNA  
694 sequences into the new bacterial taxonomy. *Appl. Environ. Microbiol.* 2007; 73: 5261-5267.

695 40 Delgado-Baquerizo M, Oliverio AM, Brewer TE, Benavent-Gonzalez A, Eldridge DJ, Bardgett RD, et  
696 al. A global atlas of the dominant bacteria found in soil. *Science*. 2018; 359: 320-325.

697 41 Kumar S, Stecher G, Li M, Knyaz C, Tamura K. MEGA X: Molecular Evolutionary Genetics Analysis  
698 across Computing Platforms. *Mol. Biol. Evol.* 2018; 35: 1547-1549.

699 42 Schloss PD, Westcott SL, Ryabin T, Hall JR, Hartmann M, Hollister EB, et al. Introducing mothur:  
700 Open-Source, Platform-Independent, Community-Supported Software for Describing and Comparing  
701 Microbial Communities. *Appl. Environ. Microbiol.* 2009; 75: 7537-7541.

702 43 Jiao S, Yang Y, Xu Y, Zhang J, Lu Y. Balance between community assembly processes mediates species  
703 coexistence in agricultural soil microbiomes across eastern China. *ISME J.* 2020; 14: 202-216.

704 44 Banerjee S, Schlaeppi K, van der Heijden MGA. Keystone taxa as drivers of microbiome structure and  
705 functioning. *Nat. Rev. Microbiol.* 2018; 16: 567-576.

706 45 Logares R, Lindstrom ES, Langenheder S, Logue JB, Paterson H, Laybourn-Parry J, et al.  
707 Biogeography of bacterial communities exposed to progressive long-term environmental change. *ISME*  
708 *J.* 2013; 7: 937-948.

709 46 Wu W, Lu H-P, Sastri A, Yeh Y-C, Gong G-C, Chou W-C, et al. Contrasting the relative importance of  
710 species sorting and dispersal limitation in shaping marine bacterial versus protist communities. *ISME*  
711 *J.* 2018; 12: 485-494.

712 47 Jabot F, Etienne RS, Chave J. Reconciling neutral community models and environmental filtering:  
713 theory and an empirical test. *Oikos*. 2008; 117: 1308-1320.

714 48 Feinstein LM, Blackwood CB. Taxa-area relationship and neutral dynamics influence the diversity of  
715 fungal communities on senesced tree leaves. *Environ. Microbiol.* 2012; 14: 1488-1499.

716 49 Guo X, Feng J, Shi Z, Zhou X, Yuan M, Tao X, et al. Climate warming leads to divergent succession of  
717 grassland microbial communities. *Nat. Clim. Chang.* 2018; 8: 813-818.

718 50 Ning D, Deng Y, Tiedje JM, Zhou J. A general framework for quantitatively assessing ecological  
719 stochasticity. *Proc. Natl. Acad. Sci. U. S. A.* 2019; 116: 16892-16898.

720 51 Grace JB, Bollen KA. Representing general theoretical concepts in structural equation models: the role  
721 of composite variables. *Environ. Ecol. Stat.* 2008; 15: 191-213.

722 52 Roy AH, Rosemond AD, Paul MJ, Leigh DS, Wallace JB. Stream macroinvertebrate response to  
723 catchment urbanisation (Georgia, USA). *Freshw. Biol.* 2003; 48: 329-346.

724 53 Wu L, Ning D, Zhang B, Li Y, Zhang P, Shan X, et al. Global diversity and biogeography of bacterial  
725 communities in wastewater treatment plants. *Nat. Microbiol.* 2019; 4: 1183-1195.

726 54 Liu L, Yang J, Yu Z, Wilkinson DM. The biogeography of abundant and rare bacterioplankton in the  
727 lakes and reservoirs of China. *ISME J.* 2015; 9: 2068-2077.

728 55 Vasquez-Ponce F, Higuera-Llanten S, Pavlov MS, Marshall SH, Olivares-Pacheco J. Phylogenetic  
729 MLSA and phenotypic analysis identification of three probable novel *Pseudomonas* species isolated on  
730 King George Island, South Shetland, Antarctica. *Braz. J. Microbiol.* 2018; 49: 695-702.

731 56 Gleeson T, Befus KM, Jasechko S, Luijendijk E, Cardenas MB. The global volume and distribution of  
732 modern groundwater. *Nat. Geosci.* 2016; 9: 161-167.

733 57 Clark DR, Underwood GJC, McGenity TJ, Dumbrell AJ. What drives study-dependent differences in  
734 distance-decay relationships of microbial communities? *Glob. Ecol. Biogeogr.* 2021; 4: 881-825.

735 58 Zhang X, Liu S, Wang J, Huang Y, Freedman Z, Fu S, et al. Local community assembly mechanisms  
736 shape soil bacterial beta diversity patterns along a latitudinal gradient. *Nat. Commun.* 2020; 11: 5428.

737 59 Hérault B. Reconciling niche and neutrality through the Emergent Group approach. *Plant Ecol. Evol.*  
738 *Syst.* 2007; 9: 71-78.

739 60 Chen J, Wang P, Wang C, Wang X, Miao L, Liu S, et al. Fungal community demonstrates stronger  
740 dispersal limitation and less network connectivity than bacterial community in sediments along a large  
741 river. *Environ. Microbiol.* 2020; 22: 832-849.

742 61 Zhou L, Li H, Zhang Y, Han S, Xu H. *Sphingomonas* from petroleum-contaminated soils in Shenfu,  
743 China and their PAHs degradation abilities. *Braz. J. Microbiol.* 2016; 47: 271-278.

744 62 Mendes LW, Kuramae EE, Navarrete AA, van Veen JA, Tsai SM. Taxonomical and functional microbial  
745 community selection in soybean rhizosphere. *ISME J.* 2014; 8: 1577-1587.

746 63 Arcese P, Sinclair ARE. The role of protected areas as ecological baselines. *J. Wildl. Manage.* 1997; 61:  
747 587-602.

748 64 Danielopol DL, Griebler C. Changing paradigms in groundwater ecology - from the 'living fossils'  
749 tradition to the 'new groundwater ecology'. *Int. Rev. Hydrobiol.* 2008; 93: 565-577.

750 65 Sirisena KA, Daughney CJ, Moreau M, Ryan KG, Chambers GK. Relationships between molecular  
751 bacterial diversity and chemistry of groundwater in the Wairarapa Valley, New Zealand. *N. Z. J. Mar.*  
752 *Freshw. Res.* 2014; 48: 524-539.

753 66 Farnleitner AH, Wilhartz I, Ryzinska G, Kirschner AKT, Stadler H, Burtscher MM, et al. Bacterial  
754 dynamics in spring water of alpine karst aquifers indicates the presence of stable autochthonous  
755 microbial endokarst communities. *Environ. Microbiol.* 2005; 7: 1248-1259.

756 67 Wang Y, Zhou S. Ar-40/Ar-39 dating constraints on the high-angle normal faulting along the southern  
757 segment of the Tan-Lu fault system: An implication for the onset of eastern China rift-systems. *J. Asian*  
758 *Earth Sci.* 2009; 34: 51-60.

759 68 Zhalnina K, Louie KB, Hao Z, Mansoori N, da Rocha UN, Shi S, et al. Dynamic root exudate chemistry  
760 and microbial substrate preferences drive patterns in rhizosphere microbial community assembly. *Nat.*  
761 *Microbiol.* 2018; 3: 470-480.

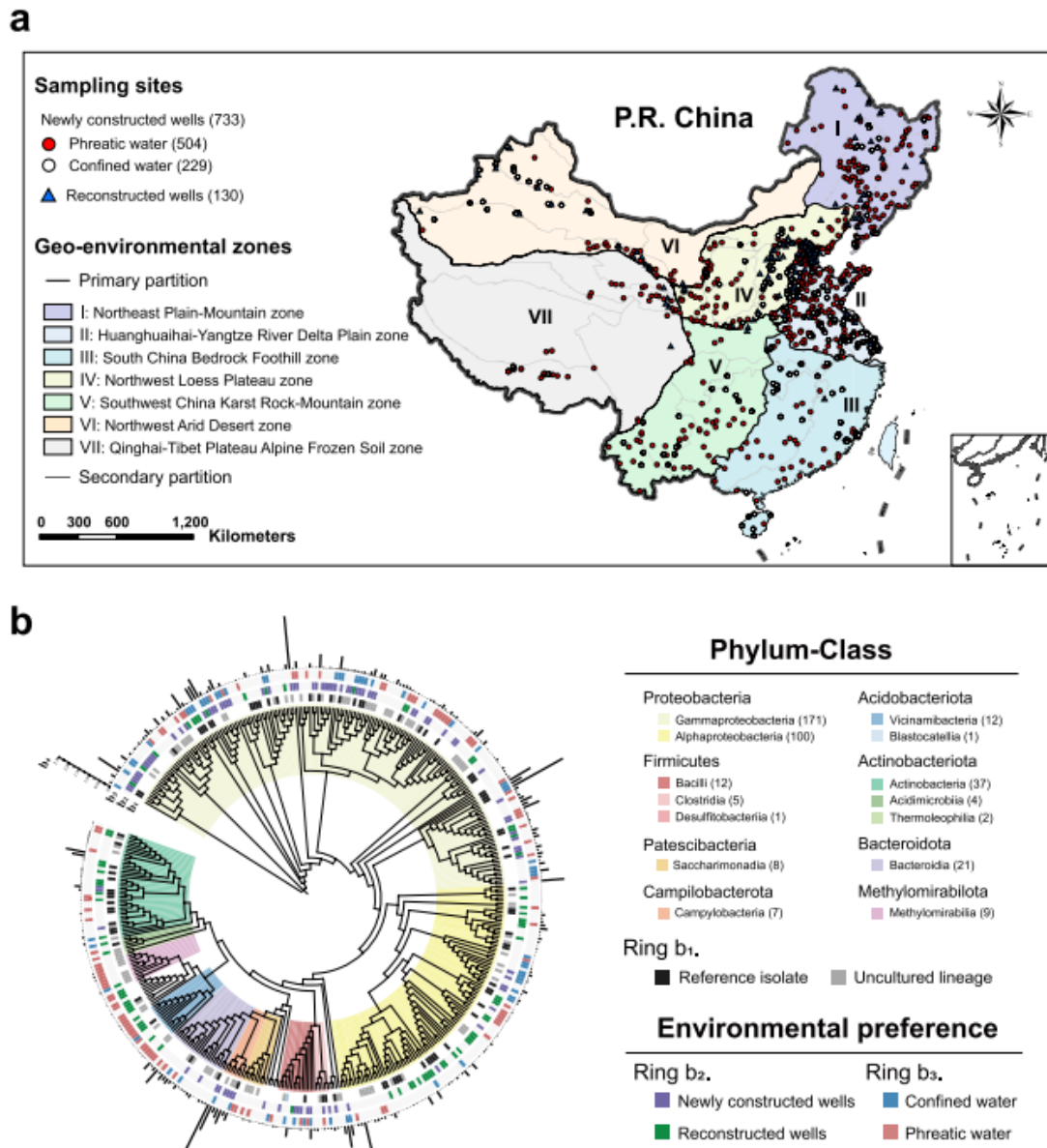
762 69 Bernard C, Lannes R, Li Y, Baptiste E, Lopez P. Rich repertoire of quorum sensing protein coding  
763 sequences in CPR and DPANN associated with interspecies and interkingdom communication.  
764 *Msystems.* 2020; 5: e00414-20.

765 70 Liu T, Zhang AN, Wang J, Liu S, Jiang X, Dang C, et al. Integrated biogeography of planktonic and  
766 sedimentary bacterial communities in the Yangtze River. *Microbiome.* 2018; 6: 16.

767 71 Hoehler TM, Jørgensen BB. Microbial life under extreme energy limitation. *Nat. Rev. Microbiol.* 2013;  
768 11: 83-94.

769 72 Castano-Sánchez A, Hose GC, Reboleira ASP. Ecotoxicological effects of anthropogenic stressors in  
770 subterranean organisms: A review. *Chemosphere.* 2020; 244: 125422.

771  
772



774

775

776

777

778

779

780

781

782

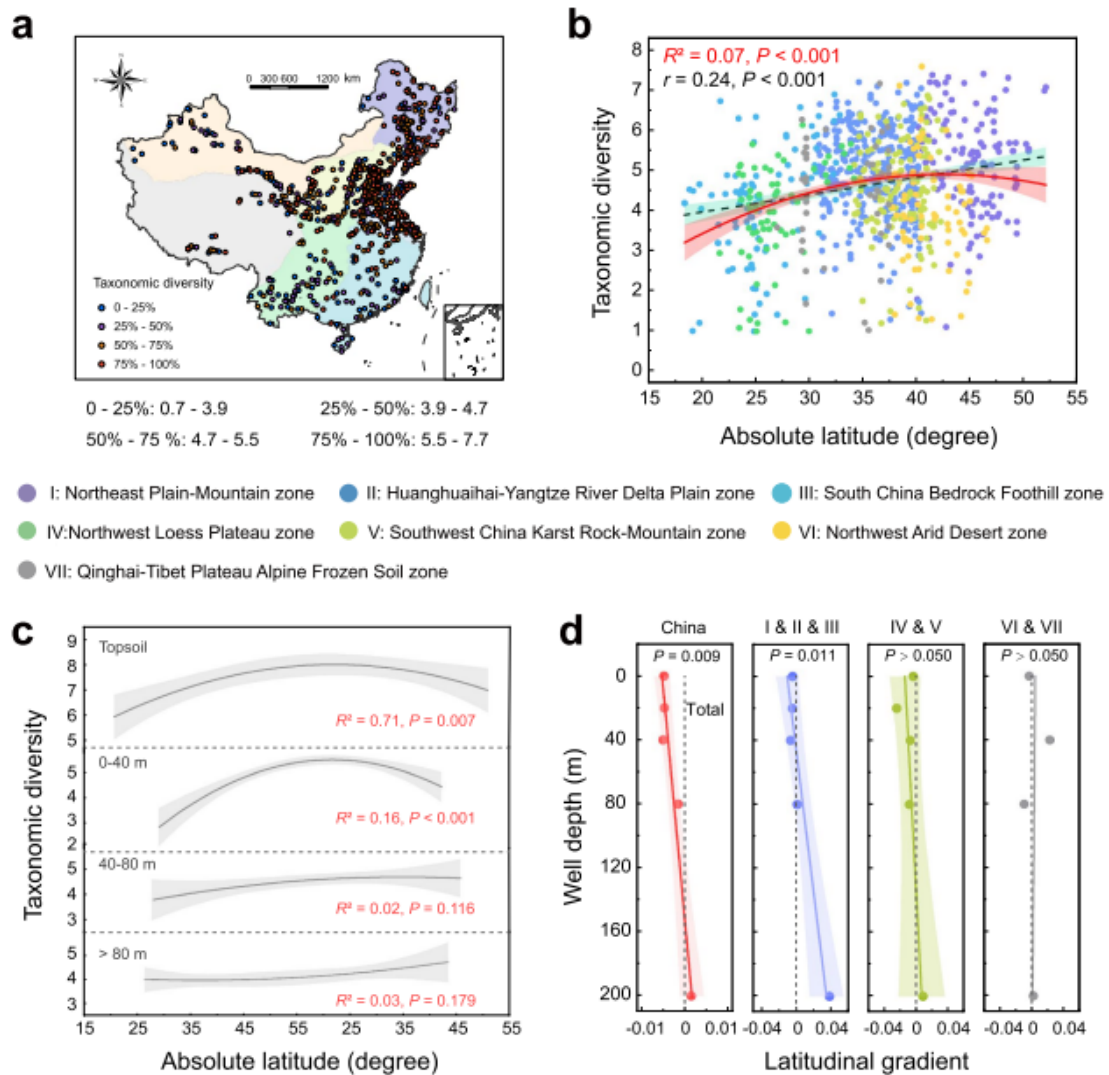
783

784

785

786

**Fig. 1** The atlas of dominant microbes in continental groundwater. a 863 sampling sites distributed throughout China. Groundwater samples collected from 733 newly constructed and 130 reconstructed wells are marked by circles and triangles. For newly constructed wells, red and white circles represent phreatic and confined groundwater samples. The background is a composite of seven geo-environmental zones. b Phylogenetic tree of core taxa in groundwater. The colors in the innermost ring indicate taxonomic information on core taxa at class level. On ring b1, black indicates a representative strain matched at the  $\geq 97\%$  similarity level, and gray indicates taxa identified as having uncultured lineage. The colors on rings b2 and b3 denote environmental preference. The histogram (b4) in the outermost ring displays average relative abundance.



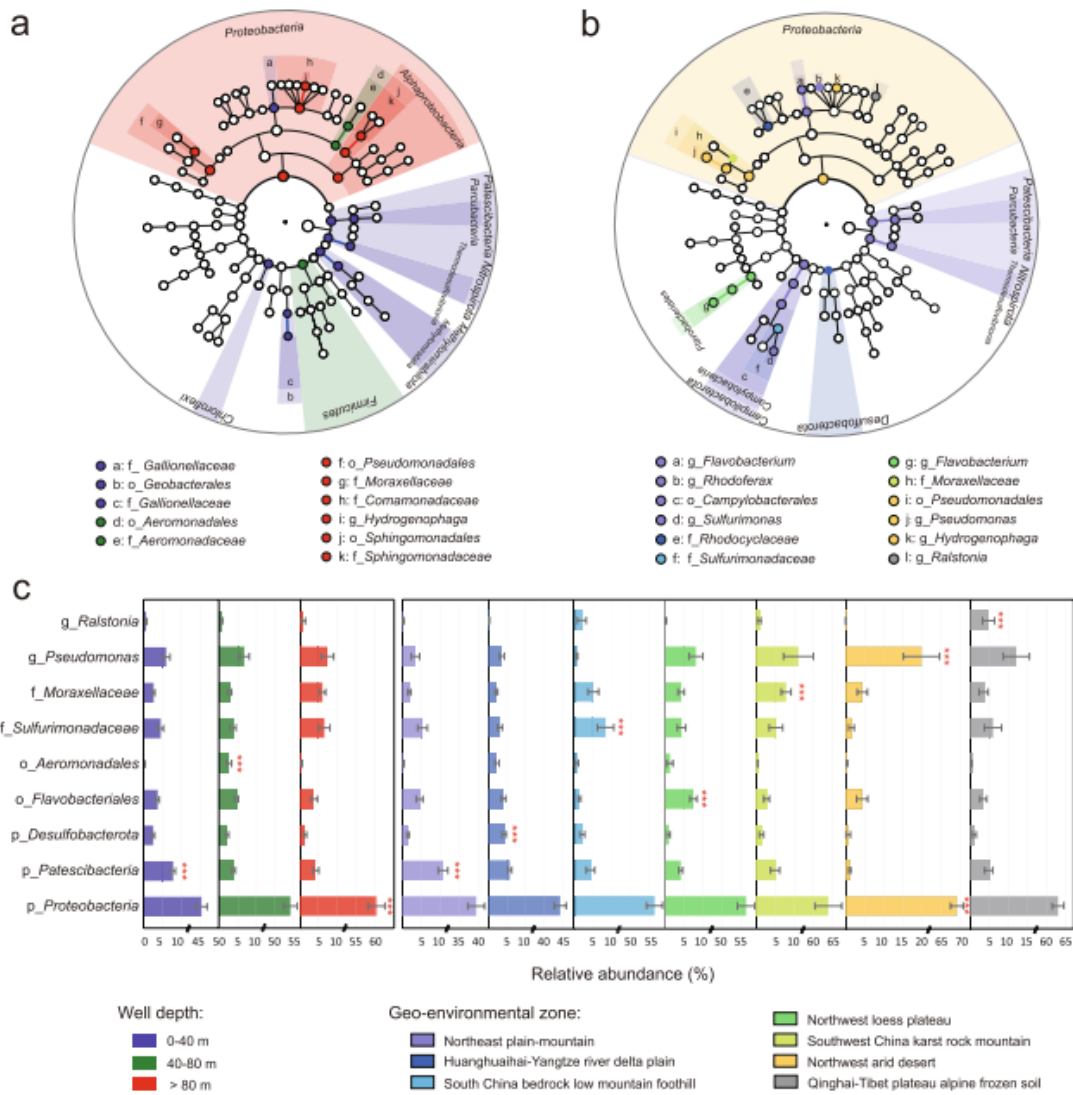
788

789

790 **Fig. 2** Biogeographic patterns of groundwater baseline microbes in China. **a** Spatial distribution of  
791 groundwater microbial diversity across seven geo-environmental zones. **b** Microbial latitudinal  
792 diversity gradient (LDG) in groundwater. Red solid and black dashed lines show polynomial and  
793 linear fits based on ordinary least square regression, with the shaded area representing 95%  
794 confidence intervals. Values of the adjusted  $R^2$  of the polynomial fits and Pearson's  $r$  of the linear fits  
795 are provided. **c** Comparison of LDG pattern in three well-depth ranges of phreatic water with that on  
796 the topsoil. **d** Vertical trend of LDG pattern in eastern (zone I, II, and III), middle (zone IV and V),  
797 and western (zone VI and VII) China. Quadratic coefficients of polynomial fits of LDG are used to  
798 represent their variation rate in varying well-depth ranges.

799

800



802

803

804

**Fig. 3** Biomarkers of varying groundwater samples. LefSe cladogram showing biomarkers of **a** three well-depth ranges and **b** varying geo-environmental zones. Abundant taxa with average relative abundance of  $\geq 0.5\%$  are assigned to kingdom (innermost), phylum, class, order, family, and genus (outermost). Each biomarker is colored by its environmental preferences. **c** Spatial distribution of representative biomarkers for depth-based microbial baselines in varying geo-environments.

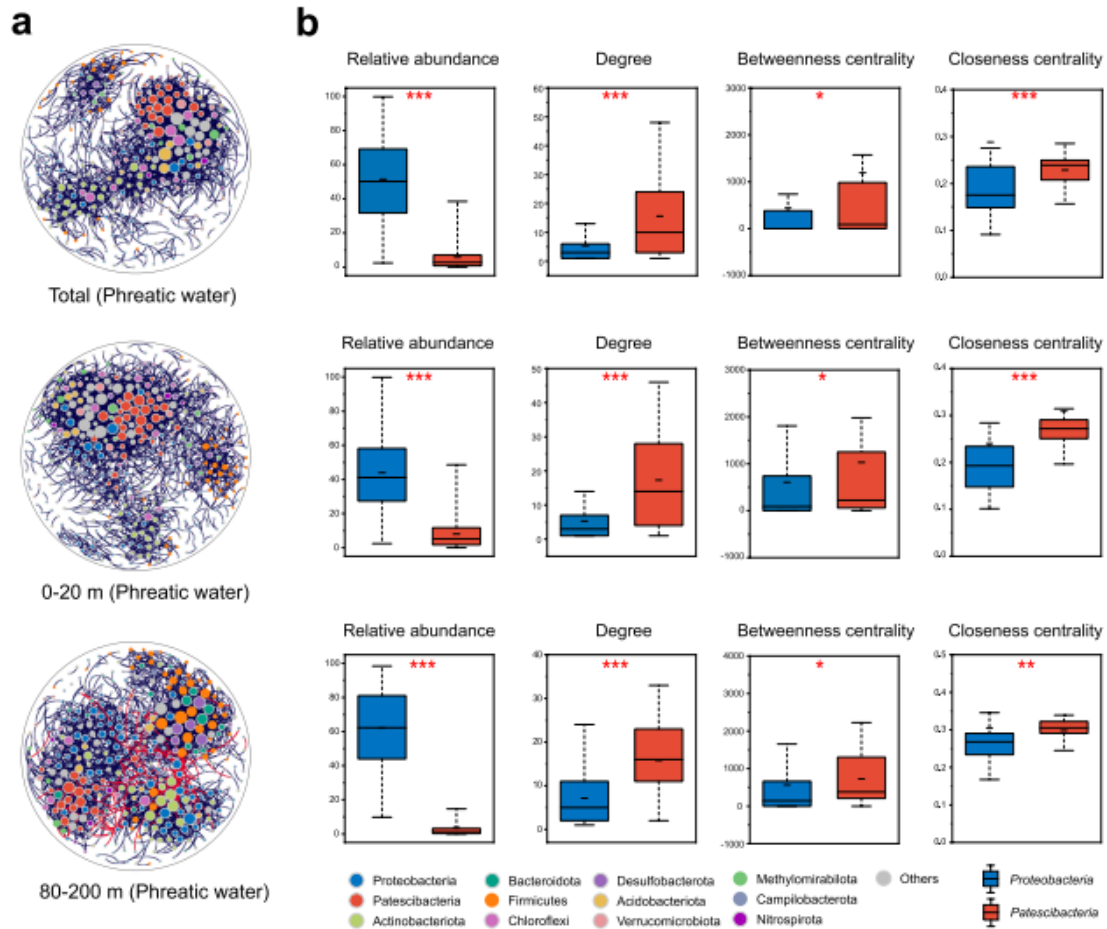
807

808

809

810

811



812

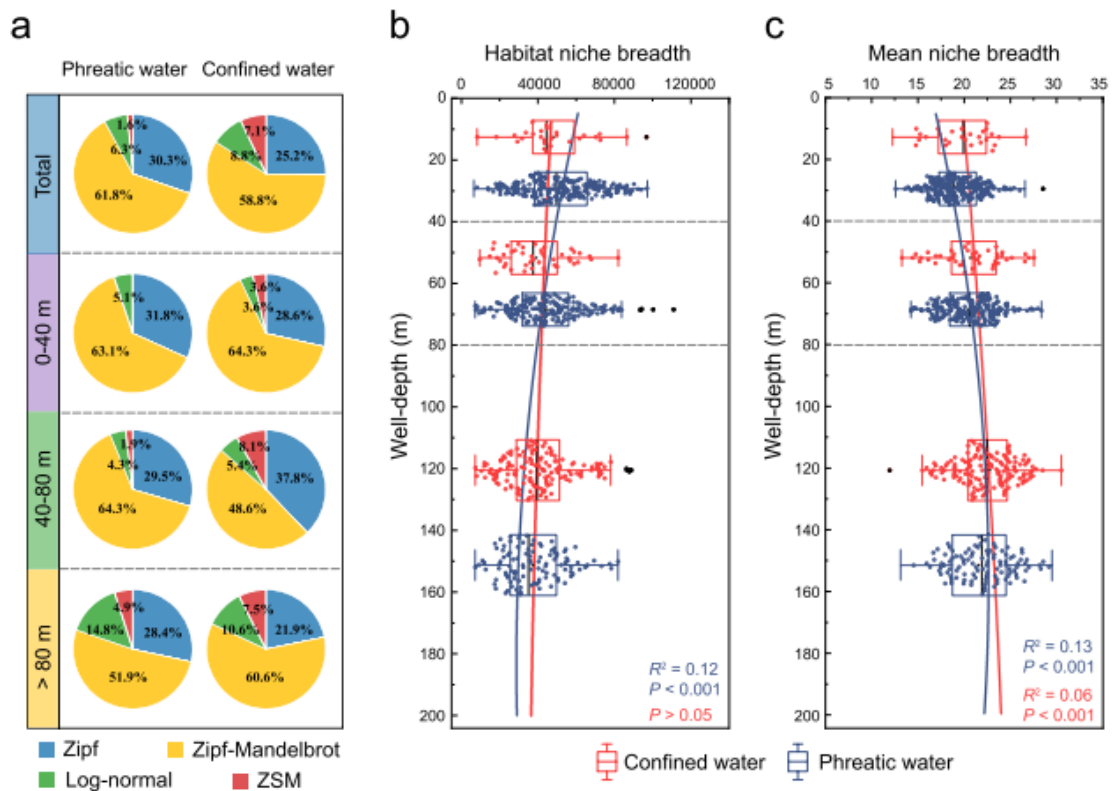
813

814 **Fig. 4** Coexistence patterns of baseline microbes. **a** Co-occurrence networks of microbial community  
 815 at genus level (average relative abundance > 0.01%) for phreatic water samples. Each node  
 816 represents one genus, and each edge represents a strong and significant correlation between two  
 817 genera (Spearman's  $|r| > 0.6$  with FDR-adjusted  $P < 0.001$ ). The size of each node is proportional to  
 818 the degree, and the phyla of nodes are labelled in distinct colors. Black and red edges indicate  
 819 positive and negative relationships. **b** Comparisons of relative abundance and node-level topological  
 820 features (degree, betweenness centrality, and closeness centrality) between Proteobacteria and  
 821 Patescibacteria. \* $0.01 < P < 0.05$ , \*\* $0.001 < P < 0.01$ , and \*\*\* $P < 0.001$

822

823





824

825

826

827

828

829

830

831

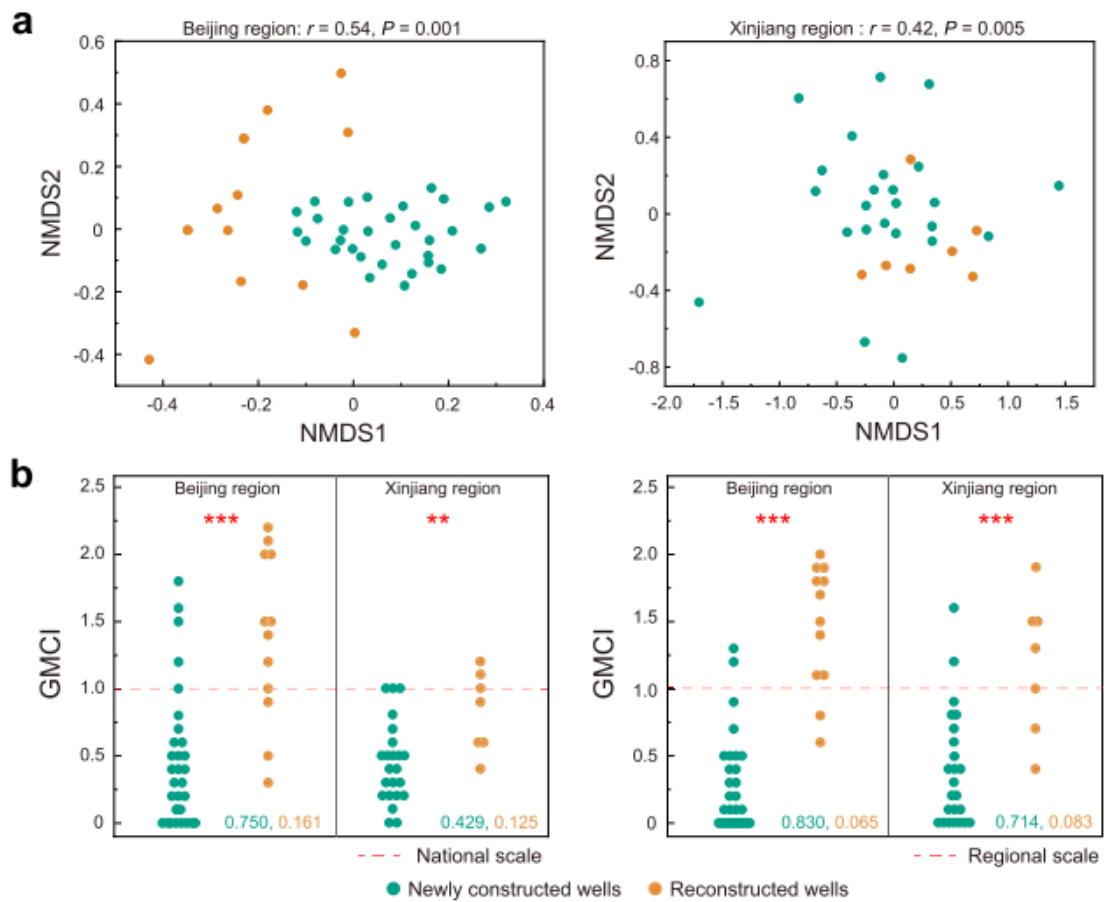
832

833

834

835

**Fig. 5** Deterministic community assembly of groundwater baseline microbes. **a** Proportions of samples fitted to pre-emption, broken stick, log-normal, Zipf, Zipf-Mandlebrot, and ZSM models at varying well-depth ranges (total, 0–40, 40–80, and > 80 m) in phreatic and confined water. ZSM was a neutral-based model, whereas the other models were niche-based. **b, c** Variations in habitat niche breadth and mean niche breadth (OTUs) of each sample with well-depth. Boxplots illustrate habitat niche breadth and mean niche breadth in phreatic (blue) and confined (red) water for varying well-depth ranges (0–40, 40–80, and > 80 m). Blue and red lines display the polynomial regression of niche breadth against well depth in phreatic and confined water.



836

837

838 **Fig. 6** Evaluation of anthropogenic interferences on groundwater bacterial communities. **a** Non-  
 839 metric multidimensional scaling (NMDS) analysis based on Bray–Curtis similarity showing  
 840 compositional discrepancy on microbial community between newly constructed and reconstructed  
 841 wells. Beijing and Xinjiang regions are selected as the representative regions suffering strong and  
 842 weak human intervention, respectively. **b** Comparisons of GMCI assessment results of microbial  
 843 communities in newly constructed and reconstructed wells. Left figure shows GMCI assessment  
 844 results of two representative regions based on national baseline data, while right one is based on  
 845 regional baseline data. The identified accurate rate (green) and error rate (yellow) are provided in the  
 846 panel legend.